# Vinculin Tail Conformation and Self-Association Is Independent of pH and H906 Protonation[†]

Sean M. Palmer,[‡] Michael D. Schaller,[§,||] and Sharon L. Campbell*[,‡,||]

*Department of Biochemistry and Biophysics, University of North Carolina at Chapel Hill, Chapel Hill, North Carolina 27599, Department of Cell and Development Biology, University of North Carolina at Chapel Hill, Chapel Hill, North Carolina 27599, and Lineberger Comprehensive Cancer Center, University of North Carolina at Chapel Hill, Chapel Hill, North Carolina 27599*

*Received September 16, 2008; Revised Manuscript Received October 3, 2008*

ABSTRACT: Vinculin is a highly conserved cytoskeletal protein that localizes to sites of cell adhesion. The tail domain of vinculin (Vt) forms tight autoinhibitory interactions with the head domain and down-regulates vinculin function by obscuring ligand binding sites. Ligand binding is required for both vinculin activation and function, and one of vinculin's primary roles as a cell adhesion protein involves its ability to link the Actin cytoskeleton to the cell membrane. Vt can bind F-Actin and phosphoinositol 4,5-bisphosphate, and association with these ligands has been reported to cause a conformational change in Vt. Moreover, a single histidine residue, H906, was reported to be critical for both a pH dependent conformational change and pH dependent self-association. In this study, we investigate the role of pH on Vt structure and self-association. In contrast to earlier observations, our studies do not support a significant alteration in Vt conformation over this pH range. Moreover, while we identify a site of Vt dimerization, similar to that observed previously by X-ray crystallography, the weak $K_d$ (~300 $\mu$M) determined for Vt self-association does not differ significantly between pH 5.5 and pH 7.5.

Contacts between cells (cell−cell) and with the extracellular matrix (cell−matrix) regulate a wide variety of critical cellular processes including cell growth, migration, differentiation and cell death (*1*−*3*). Aberrant regulation of these processes contributes to a number of human diseases, including cancer (*4*). The highly conserved cytoskeletal protein, vinculin, is found in both cell−cell and cell−matrix contacts (*5*), is essential for embryogenesis (*6*), and plays an important role in regulating cell morphology and migration (*7*). Vinculin is a large, approximately 116 kDa protein consisting of an amino-terminal head domain (~90 kDa) and a carboxy-terminal tail domain (~21 kDa) connected by a flexible hinge region. The vinculin tail (Vt[1]) domain forms autoinhibitory contacts with the vinculin head (Vh) domain and binds several ligands including F-Actin, paxillin, PKCα and acidic phospholipids (*8*−*15*). Intramolecular contacts between the head and tail domain are released for vinculin activation, as these autoinhibitory contacts prevent the interaction of multiple ligands (*11*−*13, 16, 17*). Current models of vinculin activation have proposed that a combinatorial input of multiple ligands is necessary to release interactions between the head and tail domain. For example, acidic phospholipid or F-Actin binding to the tail domain, when coupled with talin association with the head domain have been shown to modulate vinculin activity (*18*−*21*). The binding of these ligands is believed to induce conformational changes in both the head and tail domains causing disruption of autoinhibitory contacts (*18, 19, 22, 23*). One study suggested that a single histidine residue (H906) in the vinculin tail domain (Vt) is critical for both a pH- and lipid-dependent conformational change in Vt, which in turn, can modulate vinculin head/tail interactions (*24*).

Several crystal structures of vinculin are now available (*18, 19, 22, 25*). The isolated Vt domain was solved at pH 5.0 and found to possess an antiparallel, five helix bundle fold. Crystal structures of full length vinculin have been solved at pH 6.5 and pH 8.0 (*18, 25*). The tail domain adopts a similar structure in the context of the full length protein, despite differences in the pH at which the structures were solved. In addition to the helix bundle fold, Vt contains an N-terminal strap (residues 879 to 893) that exists in an extended conformation and packs against the helix bundle forming interactions with residues along the helix 1−2 face and C-terminus. In particular, the side chain of strap residue F885 packs against the H906 side chain in helix 1, and strap residue D882, forms electrostatic interactions with S914, K924, K1061, and Y1065. These residues are located in the loop between helices 1 and 2, helix 2, and the C-terminus, respectively. The N-terminal strap is observed in multiple

[†] This work was supported by National Institutes of Health Grant HL45100 (to M.D.S. and S.L.C.).

* To whom correspondence should be addressed. Phone: 919-966-6781. Fax: 919-966-2852. E-mail: sharon_campbell@med.unc.edu.

[‡] Department of Biochemistry and Biophysics.

[§] Department of Cell and Development Biology.

[||] Lineberger Comprehensive Cancer Center.

[1] Abbreviations: AUC, analytical ultracentrifugation; BME, β-mercaptoethanol; CD, circular dichroism; DTT, dithiothreitol; EDTA, ethylenediaminetetraacetic acid; GdmCl, guanidinium chloride; HSQC, heteronuclear single quantum coherence; IPTG, isopropyl-beta-D-thiogalactopyranoside; $K_d$, dissociation constant; NMR, nuclear magnetic resonance; PKCα, protein kinase C-α; TCEP, Tris(2-carboxyethyl)phosphine; Tris, tris(hydroxymethyl)aminomethane; UV, ultraviolet; Vt, the tail domain of vinculin.

10.1021/bi801764a CCC: $40.75 
Published on Web 11/04/2008

conformations in the crystal structure of isolated Vt and thus may possess conformational mobility.

Histidine 906 has been implicated in both pH- and lipid-induced Vt conformational changes, which in turn affect autoinhibitory contacts between the head and tail domain (*24*). To better characterize the role of H906 in pH-dependent Vt conformational changes, we investigated whether the protonation state of H906 influences Vt structure using NMR and CD spectroscopy. Although a previous CD study indicated that protonation/deprotonation of H906 promotes a change in Vt conformation (*24*), results obtained from our NMR and CD studies do not support a sizable conformational change in Vt over a pH range from 5.5 to 7.5. In particular, NMR spectral comparison of the Vt variant, H906A, show localized chemical shift perturbations in helix 1, helix 2 and the N-terminal strap compared to wild-type Vt, consistent with perturbation of the F885/H906 interaction resulting in the release of the strap from the helix 1−2 interface. However, loss of this contact does not appear to cause a sizable conformational change in the Vt helix bundle fold. As H906 has also been implicated in pH-dependent Vt self-association (*24*), we employed NMR and analytical ultracentrifugation (AUC) to investigate whether Vt undergoes pH-dependent self-association. The isolated Vt domain was crystallized as a dimer at pH 5.0, with the site of dimerization located in the upper portions of helices 4 and 5 (*19*). Our NMR and AUC data support Vt self-association in the solution state, with the dimerization interface consistent with that observed by crystallography. However, in contrast to a previous report (*24*), our results indicate that Vt does not undergo a monomer to dimer transition between pH 5.5 and pH 7.5. Thus, our results indicate that Vt does not undergo a pH-dependent change in structure and retains a similar ability to self-associate between pH 5.5 and pH 7.5.

## EXPERIMENTAL PROCEDURES

*1. Protein Expression and Purification.* The tail domain of chicken vinculin (Vt), residues 879−1066 (98.9% identity with human vinculin), was expressed with a N-terminal His-tag (*19*). The Vt construct was transformed into *E. coli* strain BL21(DE3) and expression of Vt induced upon addition of 0.25 mM isopropyl-$\beta$-D-thiogalactopyranoside (IPTG) at 37 °C. Cells were grown for 5 h and lysed by sonication in a buffer containing 20 mM Tris, pH 7.5, 150 mM NaCl, 5 mM Imidizole, and 0.1% $\beta$-mercaptoethanol (BME). Soluble protein was separated by centrifugation, for 1 h at 25,000 *g*. Vt was initially purified by affinity separation using Ni-NTA Agarose beads (Qiagen). The bound protein was washed and eluted with lysis buffers containing 60 mM and 500 mM imidizole, respectively. The eluted protein was dialyzed into thrombin cleavage buffer (20 mM Tris, pH 7.5, 500 mM NaCl, 2.5 mM $CaCl_2$, and 0.1% BME) and the His-tag was cleaved by incubation with thrombin (~1 unit per 5 mg protein) overnight at 37 °C. The cleaved His-tag was then removed by dialysis in the same buffer. Vt was then further purified by cation-exchange chromatography (HiPrep 16/10 SP XL column, GE Healthcare Life Sciences) in a buffer containing 20 mM Tris (pH 7.5), 2.5 mM ethylenediaminetetraacetic acid (EDTA), and 0.1% BME, with a 0.05−1 M NaCl gradient. In some cases, insoluble Vt was refolded and purified by resuspending cell pellets in 6 M guanidinium chloride (GdmCl) prior to sonication. GdmCl-treated Vt was purified using a procedure similar to that for soluble Vt, except that purification using Ni-NTA agarose beads was carried out under denaturing conditions. Vt was subsequently refolded upon removal of the GdmCl by dialysis in a buffer containing 20 mM Tris, pH 7.5, 500 mM NaCl, and 0.1% BME. The His-tag was removed and Vt further purified by cation-exchange chromatography, using the procedures described above for the natively folded protein. $^1H-^{15}N$ HSQC NMR spectra were acquired on $^{15}N$-enriched refolded Vt and natively folded Vt to verify similar spectral features and proper refolding. The Vt mutant, Vt H906A, was expressed and purified using procedures described above for wild-type Vt.

*2. Nuclear Magnetic Resonance Assignments.* Nuclear magnetic resonance (NMR) assignments were obtained for the majority of wild-type Vt backbone $^1H_N$, $^{15}N$, $^{13}C_\alpha$, $^{13}CO$, and side chain $^{13}C_\beta$ resonances. The assignments and associated experimental details, have been reported (*26*) and are deposited in the Biological Magnetic Resonance Data Bank (http://www.bmrb.wisc.edu/), accession number 15653. Briefly, NMR assignments were determined using a standard series of triple resonance experiments ($^1H-^{15}N$ HSQC, HNCO, HN(CA)CO, HNCA, HNCACB, HN(CA)CB, HN(CO)CA, and HN(COCA)CB) (*27*) on ($^2H$, $^{13}C$, $^{15}N$)-enriched Vt in a buffer containing 10 mM $K_2HPO_4$, 50 mM NaCl, 0.01% $NaN_3$, 2 mM dithiothreitol (DTT) at pH 5.5, in 90% $H_2O$, and 10% $D_2O$. NMR resonance assignments for Vt H906A were determined using assignments of wild-type Vt as a starting point, along with analyses of 3D HNCO, HNCA, and HN(CA)CB spectra on ($^{13}C$, $^{15}N$)-enriched labeled Vt H906A.

*3. NMR Samples. E. coli* strain BL21(DE3), containing the Vt construct (*19*), were grown in minimal media containing 1 g/L $^{15}N$-$NH_4Cl$ (Spectra Stable Isotopes). Vt protein was expressed and purified as described above and exchanged into NMR buffer (10 mM potassium phosphate, 50 mM NaCl, 2 mM DTT, 0.1% $NaN_3$ and 10% $D_2O$) using an Amicon Ultra centrifugal filter device (10000-Da molecular weight cutoff, Millipore). Vt protein concentration was determined by UV absorbance (280 nm, $\varepsilon = 17990\ M^{-1}\ cm^{-1}$).

*4. NMR Spectroscopy.* NMR experiments were conducted on a Varian INOVA 700 MHz spectrometer at 37 °C. $^1H-^{15}N$ HSQC spectra were collected on uniformly $^{15}N$-enriched wild-type and Vt H906A in NMR buffer (10 mM potassium phosphate, 50 mM NaCl, 2 mM DTT, 0.1% $NaN_3$ and 10% $D_2O$), over a pH range from 5.5 using 7.5 on 150 $\mu$M protein samples. $^1H-^{15}N$ HSQC spectra were also collected on 75−1200 $\mu$M Vt samples in an identical NMR buffer (pH 5.5) to assess self-association. The data was processed with NMRPipe (*28*) and analyzed with NMRView (*29*). Weighted chemical shifts were calculated using the following equation:

$$\text{weighted chemical shift} = \sqrt{(^1H \text{ chemical shift})^2 + \frac{(^{15}N \text{ chemical shift})^2}{6}}$$

*5. Circular Dichroism.* All circular dichroism (CD) data were collected using an Applied Photophysics Pistar-180 spectrometer. The CD buffer contained 10 mM potassium

phosphate, 50 mM $Na_2SO_4$, 1 mM DTT, at either pH 5.5 or 7.5 and 25 °C. Far-ultraviolet (UV) CD spectra (260−190 nm) were collected at protein concentrations of 5 $\mu$M, while near-UV CD spectra (350−250 nm) required higher 450 $\mu$M concentration samples. In both cases, spectra were recorded in 0.5 nm steps, averaging over 100,000 samplings per step. A smoothing function using a three point window was applied to all spectra.

*6. Analytical Ultracentrifugation.* Sedimentation equilibrium experiments were performed using a Beckman Optima XL-I analytical ultracentrifuge equipped with absorbance optics. A Ti50 8-hole rotor was used with six-sectored centerpieces. Wild-type Vt and Vt H906A, each at three different concentrations (150 $\mu$M, 300 $\mu$M, and 450 $\mu$M), were analyzed at both pH 5.5 and pH 7.5 in a buffer containing 10 mM potassium phosphate, 150 mM NaCl, and 1 mM Tris(2-carboxyethyl)phosphine (TCEP). Because of high absorbance at 280 nm, data were collected at 305 nm (absorbance of all samples was between 0.2 and 0.95). The molar extinction coefficient ($\varepsilon_{305}$) was calculated from the known concentration of each samples and the absorbance at 305 nm. The $\varepsilon_{305}$ for all samples was averaged for use in further calculations. Samples were spun at 20 °C, at 19,000 rpm for 18 h, and absorbance scans were recorded every 2 h. Equilibrium was assumed to have been reached when the difference between two consecutive absorbance profiles was zero. The meniscus-depletion method was used to determine absorbance offsets after centrifugation of the samples at 40,000 rpm for 6 h (*30*). The data was fit using WinNonlin (V1.06, D. Yphantis, University of Connecticut, Storrs, CT; M. Johnson, University of Virginia, Charlottesville, VA; J. Lary, National Analytical Ultracentrifugation Facility Center), with the $K_d$ and 95% confidence interval determined by a combined fit of the 150 $\mu$M, 300 $\mu$M, and 450 $\mu$M samples. The reduced molecular mass, partial specific volume, and solvent density were calculated using Sednterp (V1.09, D. Hayes, Magdalen College, Warner, NH; T. Laue, University of New Hampshire, Durham, NH; J. Philo, Alliance Protein Laboratories).

## RESULTS

The tail domain of vinculin (Vt) has been reported to undergo an H906-dependent conformational change as a function of pH and acidic phospholipid binding (*24*). Intriguingly, H906 has also been linked to pH dependent Vt self-association (*24*). On the basis of these findings, it was speculated that H906 plays a key role in the conformational dynamic properties of Vt and thus in the regulation of vinculin function. To this end, we have employed NMR, CD, and AUC approaches to better characterize the role of H906 in pH-dependent Vt conformational changes.

*1. Mutation of Histidine 906 to Alanine Does Not Significantly Alter Vt Structure.* As mutations have the potential to alter protein structure and therefore significantly change the interpretation of experimental results, we employed CD and NMR spectroscopy to determine whether mutation of histidine 906 to alanine alters the conformation of Vt. Circular dichroism (CD) spectroscopy was employed for these analyses, as it can be used to probe both secondary and tertiary structural alterations in proteins (*31*). Far-UV (190−250 nm) CD is sensitive to the conformation of the peptide bond and therefore secondary structure of proteins and is often used to estimate the percent of secondary structure (i.e., α-helix or $\beta$-sheet) present, whereas near-UV (250−350 nm) CD can be used to detect aromatic side chain packing interactions in proteins and is thus a useful probe of tertiary structure (*31*). As shown in Figure 1, virtually identical near- and far-UV CD spectra were obtained for wild-type Vt and the Vt H906A variant at pH 7.5, indicating that both the overall helical content and the tertiary packing of aromatic residues in Vt are not significantly altered by mutation of histidine 906 to alanine.

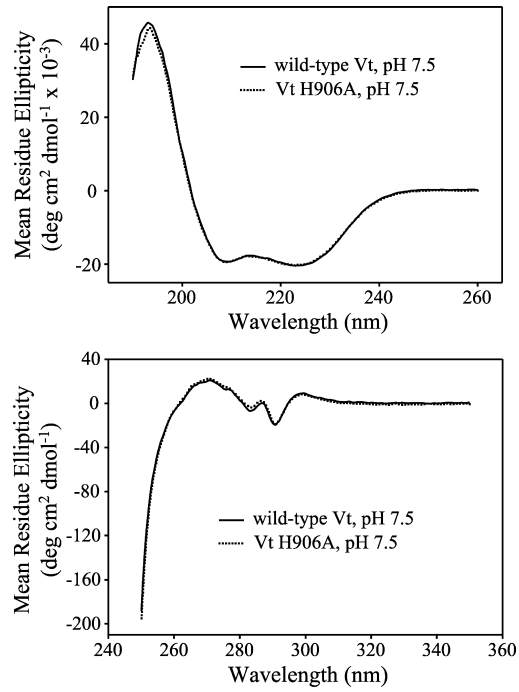


FIGURE 1: Circular dichroism (CD) spectra of wild-type Vt and Vt H906A were compared to assess whether the H906A mutation alters the secondary and/or tertiary structure. The far- (top) and near-UV (bottom) spectra of Vt and Vt H906A are virtually identical at pH 7.5, suggesting that mutation of histidine 906 to alanine does not alter the secondary or tertiary structure of Vt at pH 7.5.

However, as near and far-UV CD provide information on the average of all chromophores that absorb at the wavelength of interest in the molecular population, it is not possible to obtain residue specific information. To more specifically characterize site specific spectral perturbations in Vt resulting from mutation of H906, we employed multidimensional heteronuclear nuclear magnetic resonance (NMR) spectroscopy. Uniformly $^{15}$N-enriched wild-type Vt and the H906A Vt proteins were expressed and purified as described in Experimental Procedures, and 2D NMR heteronuclear correlation spectra collected. $^1$H−$^{15}$N heteronuclear single quantum coherence (HSQC) spectra display signals for protons attached to $^{15}$N nuclei and can provide a residue specific probe for each NH pair in wild-type and H906A Vt, as the NH resonance is sensitive to changes in its electrochemical environment. By analyzing the chemical shift and/or intensity change in NH resonances corresponding to each residue, perturbations resulting from the mutation (Vt H906A) can be assessed. A 2D $^1$H−$^{15}$N HSQC overlay of uniformly $^{15}$N-enriched wild-type and H906A Vt is shown in Figure 2. Whereas the majority of resonances are unaffected by the mutation, a small subset of NH peaks exhibit chemical shift changes greater than 0.1 ppm, with

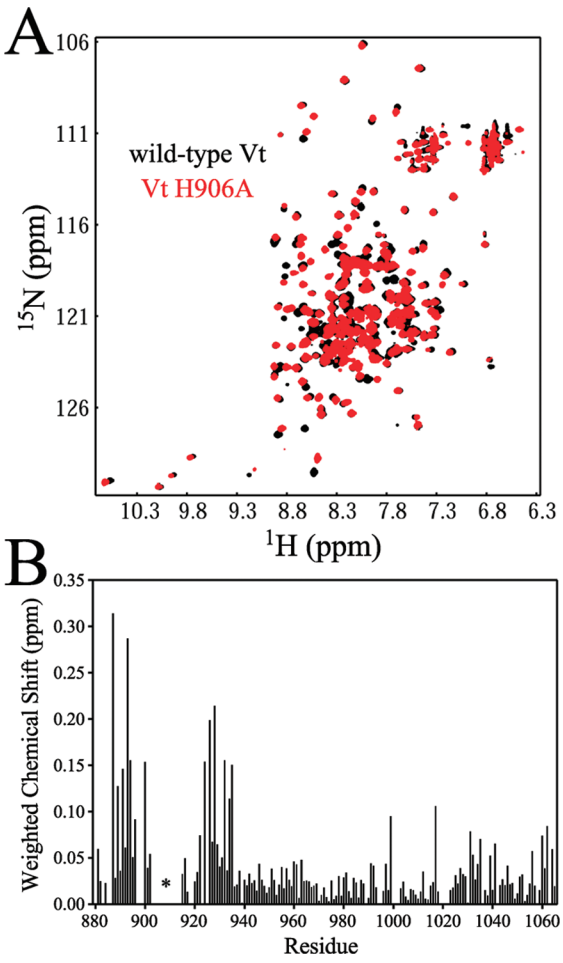


FIGURE 2: To characterize site specific spectral perturbations in Vt resulting from mutation of H906, $^{1}$H−$^{15}$N heteronuclear single quantum coherence (HSQC) spectra were collected on $^{15}$N-enriched Vt and Vt H906A (0.15 mM protein, pH 5.5). As shown in A, minor chemical shift perturbations are observed primarily for backbone HN resonances associated with residues in the N-terminal strap and the helix 1−2 interface. While these results suggest that the H906A mutation perturbs interactions with the strap, the overall fold of Vt appears unaltered. The weighted chemical shift changes for each residue are displayed in B. The majority of residues exhibit perturbations of <0.05 ppm, with perturbations >0.1 ppm localized to the N-terminal strap and the helix 1−2 interface (see Figure 3). (*) The backbone HN resonances of residues 904−914 are not detectable, presumably due to exchange broadening.

four additional NH resonances exhibiting significant loss of intensity. The residues associated with these NH resonances are contained within the N-terminal strap of Vt and the surface of helices 1 and 2 that contact the strap. These affected residues are proximal to the site of mutation (H906) in the three-dimensional structure and are displayed in Figure 3. In crystal structures of Vt and full length vinculin, H906 packs against the side chain of the N-terminal strap residue, F885. It is likely that this interaction is disrupted by mutation of the histidine aromatic side chain, resulting in the loss of contacts between the strap and helix 1, consistent with the chemical perturbations observed at these sites.

*2. The Conformation of Vt Is Largely Unaltered between pH 5.5 and 7.5.* It was previously reported that Vt undergoes a pH dependent conformational change. However, this study employed far-UV CD, which is sensitive only to the secondary structure (*24*). To assess the effects of pH changes on the secondary and tertiary structures of Vt, both near-

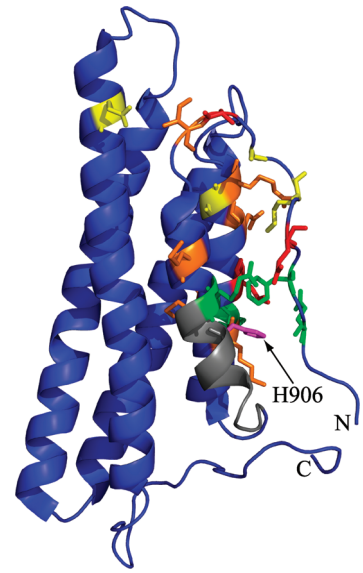


FIGURE 3: Residues exhibiting either chemical shift perturbations or significant changes in intensity due to the H906A mutation are highlighted on the structure of Vt (pdb 1ST6). The site of mutation (H906) is highlighted in magenta. Residues showing chemical shift changes >0.2 ppm, between 0.15 and 0.2 ppm, and between 0.1 and 0.15 ppm are shown in red, orange, and yellow, respectively. Residues displayed in green exhibit significant changes in either the intensity or line width of their associated NH resonances. The residues colored gray could not be measured in either wild-type Vt or Vt H906A, presumably due to exchange broadening. Almost all Vt H906A NH resonances, which demonstrate significant chemical shift or intensity perturbations relative to wild-type Vt, are localized to residues within the N-terminal strap and the surface of helices 1 and 2 that contact the strap. These results are consistent with a localized change in the N-terminal strap of Vt, but with the overall conformation of the helical bundle largely unaltered.

and far-UV CD spectra were acquired on wild-type Vt and Vt H906A at pH 5.5 and 7.5. Inspection of Figure 4, shows virtually identical near- and far-UV CD spectra at pH 5.5 and 7.5 for both Vt and Vt H906A, suggesting that neither the secondary or tertiary structure of Vt or Vt H906A differs between pH 5.5 and pH 7.5. As noted previously, CD does not provide residue specific information. To complement CD analyses, NMR studies were conducted.

$^{1}$H−$^{15}$N HSQC spectra were collected at pH values ranging from 5.5 to 7.5 for both Vt and Vt H906A. The chemical shift perturbations for all detectable resonances were analyzed with the results shown in Figure 5. For both wild-type and H906A Vt, the largest chemical shift change was observed for the H1025 NH resonance. Almost all other significant perturbations (>0.15 ppm) were from residues close to H1025, while the vast majority of resonances showed no significant perturbation (<0.1 ppm). Thus, our NMR and CD data indicate that neither the conformation of wild-type Vt nor that of Vt H906A is significantly altered between pH 5.5 and 7.5. On the basis of the small and localized nature of the chemical shifts around H1025, it is likely that these chemical shift perturbations simply represent the protonation/deprotonation of the histidine side chain rather than a localized conformational change. We could not detect and therefore assign NH resonances close to and including H906 (904−914), presumably due to broadening of these resonances by conformational exchange on the intermediate NMR time scale. However, our findings that the NH resonances corresponding to E884, K924, A927, and L928,

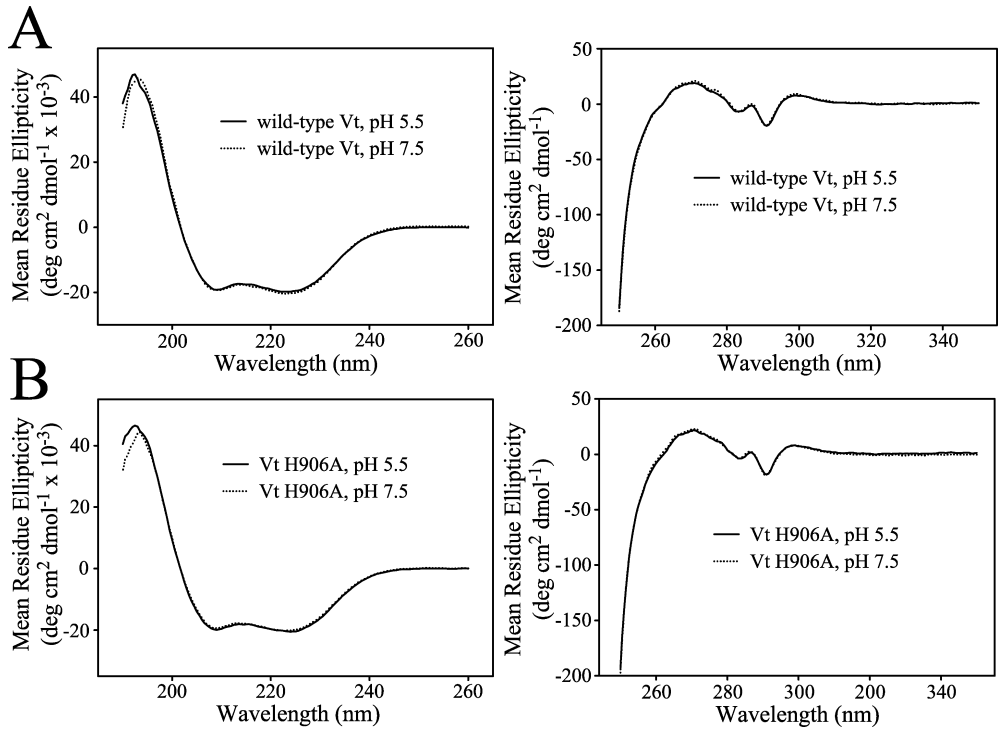


FIGURE 4: Comparison of far- (left) and near-UV (right) spectra for both wild-type Vt and Vt H906A at pH 5.5 and 7.5. CD spectra for wild-type Vt (A) and Vt H906A (B) at pH 5.5 and 7.5 are virtually identical, suggesting no significant pH-dependent conformational change for either wild-type Vt or Vt H906A over this pH range.

which are proximal to this site (904−914), do not significantly change as a function of pH indicates that either H906 does not titrate over this pH range due to interactions with the strap or that deprotonation of this side chain does not significantly alter the structure of the helix bundle.

*3. Vinculin Tail Self-Association.* Evidence for vinculin tail domain dimerization and oligomerization has been observed in both the presence and absence of F-Actin and acidic phospholipids (*19, 24, 32, 33*). As noted earlier, the vinculin tail domain was crystallized at pH 5.0 as a dimer (*19*). Moreover, studies by Miller et al. (*24*) indicate that Vt undergoes pH-dependent self-association with H906 playing a critical role. To better characterize Vt self-association and the role of H906 in this pH dependence, we have conducted NMR and analytical ultracentrifugation (AUC) studies.

$^1$H−$^{15}$N HSQC 2D NMR spectra of $^{15}$N-enriched Vt were collected over a range of protein concentrations to assess both the site of self-association and the affinity. Concentration dependent amide proton chemical shift perturbations were measured between 75 and 1200 $\mu$M Vt (Figure 6). As shown in Figure 6B and C, all residues exhibiting chemical shift changes >0.075 ppm are located in helices 4 and 5. The largest chemical shift changes correspond to residues located in the upper portion of helices 4 and 5, indicating a site of interaction similar to that observed for the Vt dimer crystal structure (*19*). The chemical shift titration data was fit to a monomer/dimer model with the majority of the shifted NH resonances giving an approximate $K_d$ between 200 and 350 $\mu$M. However, interpretation of chemical shift changes can be complicated by exchange broadening and extrapolations due to the high protein concentrations required for NMR. To better quantify Vt self-association for both wild-type Vt and Vt H906A at pH 5.5 and 7.5, AUC studies were also conducted at concentrations ranging from 150 to 450 $\mu$M. All data were fit to a monomer/dimer model of self-association. A representative monomer/dimer fit is shown in Figure 7, with apparent $K_d$ values listed in Table 1. Interestingly, Miller et al. employed gel filtration chromatography, and reported that Vt was predominately monomeric at pH 7.0 but self-associated at pH 5.5 (*24*). However, the concentrations of Vt used in these gel filtration studies were not reported, and no quantitative analysis of self-association was conducted. In contrast, results from our AUC analyses indicate that Vt is capable of self-association at both pH 5.5 and 7.5, with a similar $K_d$ of 336 and 337 $\mu$M, respectively. AUC analysis of the Vt H906A variant was also conducted at both pH 5.5 and 7.5, with $K_d$ values (323 and 286 $\mu$M at pH 5.5 and 7.5, respectively) similar to that observed for wild-type Vt.

## DISCUSSION

Ligand binding to both the vinculin head and tail domain has been reported to induce conformational changes in vinculin that facilitate vinculin activation and modulate its function (*19, 22, 33, 34*). In particular, binding of F-Actin and acidic phospholipids to the tail domain cause both a change in conformation and oligomerization state (*19, 33*). Moreover, results from studies reported by Miller and Ball supported a H906-dependent conformational change in Vt in response to pH changes and acidic phospholipid binding (*24*). According to this study, the protonation state of H906 was also reported to modulate Vt self-association. To better understand the role of H906 in pH-dependent Vt conformation and self-association, we conducted a series of biophysical studies on Vt and a variant of Vt containing an alanine substitution at H906.

H906 was previously proposed as a critical residue in lipid and pH-dependent Vt conformational changes (*24*) based on far-UV CD studies of wild-type Vt and Vt H906A. Given

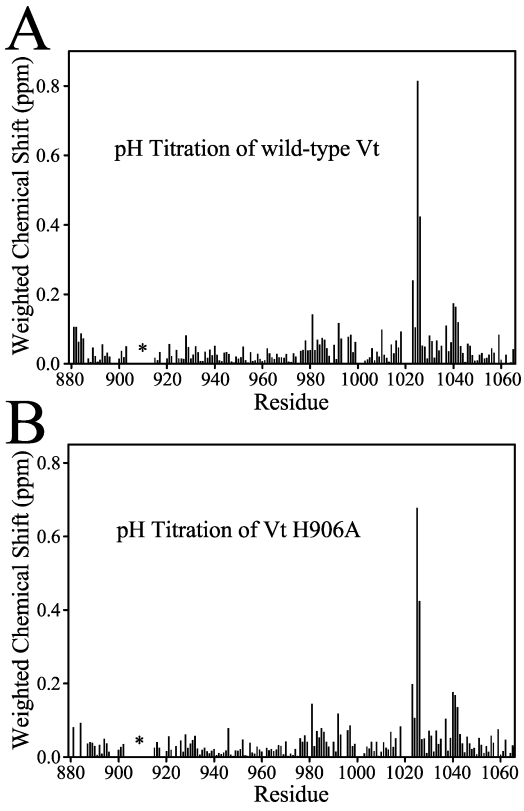


FIGURE 5: Weighted chemical shift changes in $^{1}H-^{15}N$ HSQC spectra of wild-type Vt (A) and Vt H906A (B) collected between pH 5.5 and 7.5. For both Vt and Vt H906A, the largest chemical shift changes measured correspond to H1025. The majority of chemical shift changes are small (<0.05 ppm), suggesting no overall change in Vt conformation between pH 5.5 and 7.5. The largest chemical shift changes are localized to H1025, consistent with titration of its side chain over this pH range. Furthermore, chemical shift changes observed for Vt H906A are nearly identical to those of wild-type Vt, indicating that the protonation state of H906 does not contribute to pH dependent spectra changes observed between pH 5.5 and 7.5. (*) The backbone HN resonances of residues 904−914 are not detectable, presumably due to exchange broadening.

that far-UV CD (190−250 nm) is sensitive only to secondary structure, we were interested in further characterizing whether mutation of H906 to alanine affects the tertiary structure of Vt. We thus extended the earlier studies on wild-type Vt and the H906A variant to include near-UV CD analyses, as near-UV CD (250−350 nm) is sensitive to differences in packing interactions associated with aromatic amino acids and therefore tertiary structure. Interestingly, both the near- and far-UV CD spectra of Vt and Vt H906A were similar at pH 7.5 (Figure 1). These results indicate that within the resolution of CD, mutation of histidine 906 to alanine does not alter the secondary or tertiary fold of Vt at pH 7.5. We also conducted NMR studies, as NMR spectroscopy can report on site specific differences in the chemical environment of residues within wild-type and Vt H906A. For these studies, $^{1}H-^{15}N$ HSQC spectra were collected on $^{15}N$-enriched wild-type Vt and Vt H906A to analyze chemical shift differences in the amide $^{15}N$ and proton resonances for Vt and Vt H906A. We found that the majority of the amide proton resonances in Vt H906A are not significantly changed from wild-type Vt, indicating that the overall conformation is not altered by the mutation (Figure 2), consistent with CD data. Of the resonances that do exhibit chemical shift changes, the changes are small and localized to the site of mutation. Of note, NMR chemical shifts are very sensitive to the surrounding chemical environment. Hence, changes in chemical shifts do not necessarily represent conformational changes. For residues in the immediate vicinity of H906, the removal of the histidine side chain is likely to alter the chemical shift associated with neighboring residues even in the absence of a conformational change. Chemical shift changes observed for residues removed from the mutation site are tenably explained by inspection of vinculin crystal structures (*18, 19, 25*). In the crystal structures of both Vt and full length vinculin, histidine 906 is located in helix 1. The histidine side chain extends away from the helical bundle and interacts with the side chain of phenylalanine 885 in the N-terminal strap of Vt (*18, 19*). The N-terminal strap, in turn, is held in an extended conformation along the interface of helices 1 and 2, via interactions involving F885 and D882. Interactions between the side chains of F885 and H906 are likely to stabilize contacts with the helix 1−2 interface and the extended conformation of the strap. Intriguingly, in the crystal structure of Vt, the strap is observed in two distinct conformations, suggesting conformational flexibility (*19*). Disruption of the interaction between H906 and F885 is likely to promote increased conformational flexibility in the strap, though additional interactions between residues in the strap and the helical bundle should still restrain the conformation of the strap to some degree. Mutation of histidine 906 to alanine should increase the conformational flexibility of the N-terminal strap, allowing increased sampling of alternate strap conformations due to disruption of contacts between the N-terminal strap and the helical bundle. These conformations are likely also sampled in the wild-type structure, albeit at lower frequency. The NMR chemical shift changes observed between the wild-type Vt and Vt H906A NH resonances are associated with the strap and the surface of helices 1 and 2, consistent with our premise that the H906A Vt variant perturbs interactions with the strap. The lack of chemical shift changes in the remaining helices of the bundle suggest that there are no significant conformational changes in helices 1 and 2, as structural alterations in these helices are likely to perturb the chemical environment of the other helices within the helical bundle.

CD studies by Miller and Ball concluded that although the conformation of Vt and Vt H906A are similar at pH 7.0, differences were observed at pH 5.5 (*24*). A change in the far-UV CD spectrum of wild-type Vt between pH 5.5 and 7.0 was interpreted as a pH dependent conformational change. In this previous study, far-UV CD spectra of Vt H906A but not wild-type Vt, were reported to be similar at both pH 7.0 and pH 5.5, suggesting that H906 was critical for a pH dependent conformational change in Vt (*24*). To further characterize this reported conformational change, we conducted both near- and far-UV CD on both wild-type Vt and Vt H906A, at pH 7.5 and pH 5.5. However, no significant differences were observed in CD spectra of Vt and Vt H906A at pH 7.5 or pH 5.5 (Figure 4). Thus, our CD results do not support a pH dependent conformational change for either wild-type Vt or Vt H906A. As these results differed from findings of Miller and Ball, we sought to corroborate these data with additional NMR studies. For these studies, $^{1}H-^{15}N$ HSQC NMR spectra were collected at pH values between 5.5 and 7.5 for both $^{15}N$-enriched wild-type

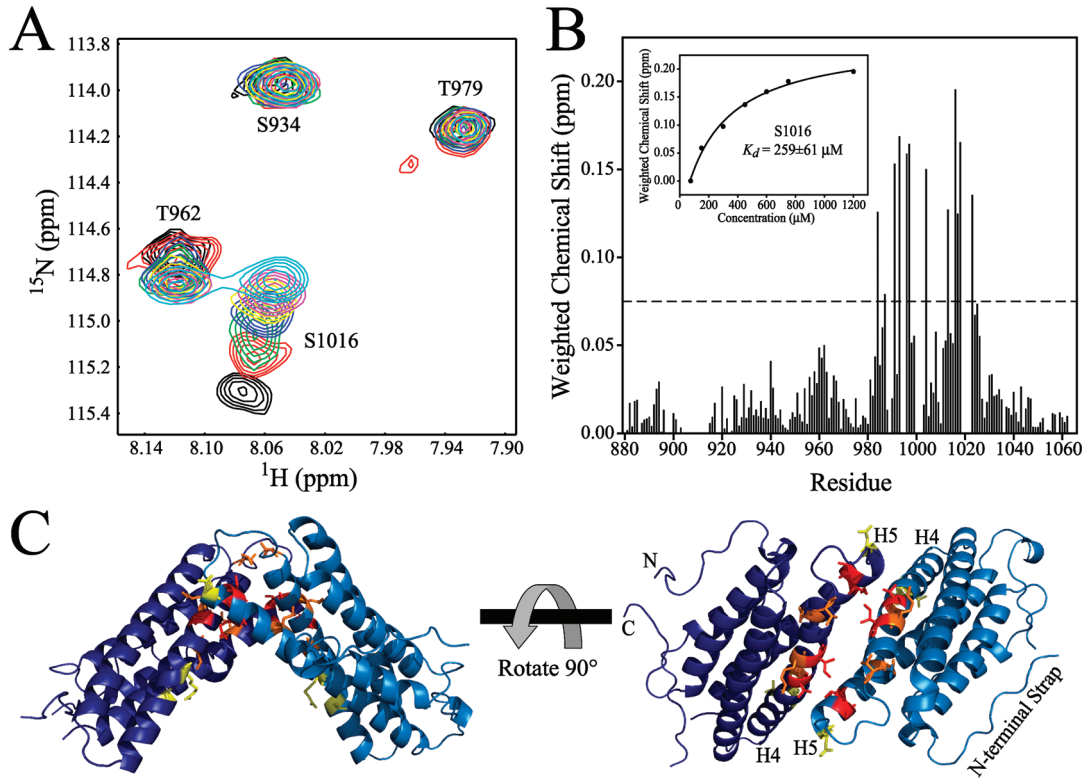


FIGURE 6: Weighted chemical shift changes observed for NH resonances detected in $^{1}$H−$^{15}$N HSQC spectra over a range of Vt concentrations between 75 and 1200 $\mu$M (pH 5.5). Panel A shows an example of an NH resonance (S1016) exhibiting concentration dependent chemical shift changes. Spectra shown in black, red, green, blue, yellow, magenta, and cyan correspond to Vt concentrations of 75, 150, 300, 450, 600, 750, and 1200 $\mu$M, respectively. Panel B shows weighted concentration dependent chemical shift changes for all measureable NH resonances between 75 and 1200 M. An example of a monomer/dimer fit is shown for S1016. In C, all residues exhibiting chemical shift changes >0.075 ppm are highlighted on the Vt dimer crystal structure (pdb 1qkr). Residues exhibiting chemical shift changes between 0.075 and 0.13 ppm, between 0.13 and 0.16 ppm, and >0.16 ppm are shown in yellow, orange, and red, respectively. All residues exhibiting chemical shift changes >0.075 ppm are located in helices 4 and 5 (H4 and H5), with all residues exhibiting major changes located within or proximal to the dimer interface.

Vt and Vt H906A. Heteronuclear 2D spectra as a function of pH provide residue specific probes of pH dependent changes. The only amino acid side chain that normally undergoes protonation/deprotonation over this pH range is that of histidine ($\delta$1 proton), consistent with our observation that the observable histidine NH resonances show the largest changes in chemical shift. Vt has two native histidine residues, H906 and H1025. Histidine 1025 exhibits large chemical shift changes over the pH range studied, consistent with the titration of its side chain. Unfortunately, the NH resonance associated with H906 is not detected in our spectra, presumably due to chemical exchange on an intermediate time scale, resulting in broadening. However, of all detectable residues, the only significant chemical shift changes are localized to H1025, likely reflecting the titration of its side chain between pH 5.5 and 7.5. Although H906 could not be measured, residues within 3−4 amino acids from H906 as well as those closest in the three-dimensional structure were detectable and showed small/insignificant chemical shift changes. Moreover, the majority of NH resonances in Vt exhibit small or indistinguishable chemical shift changes between pH 5.5 and 7.5 (Figure 5). Thus, our NMR data is consistent with CD data and provides additional evidence that the conformation of Vt is not significantly altered over this pH range. Additionally, the pH dependent chemical shift changes observed in HSQC spectra of both Vt and Vt H906A are virtually identical, indicating that mutation of H906 does not alter pH dependent Vt NMR spectral changes.

Vinculin tail self-association has been reported under a variety of different conditions by a number of groups (*8, 19, 24, 32, 33*). In one report (*24*), Vt was reported to exist in its monomeric state at pH 7.0, but self-associate at pH 5.5. In contrast, the Vt H906A variant was reported be insensitive to pH dependent self-association. On the basis of these findings, H906 was proposed to play an important role in Vt self-association. The crystal structure of Vt was solved as a dimer (*19*), with H906 distal from the site of dimerization, raising the question of how H906 could regulate this self-association. As self-association is likely critical for the F-Actin bundling function of Vt (*8, 32, 33*), we conducted NMR and AUC analyses to further characterize Vt self-association in solution. Concentration dependent NMR spectral changes observed over a concentration range of 75 to 1200 $\mu$M, support the presence of a Vt dimer at both pH 5.5 and pH 7.5. The amide proton resonances, which exhibit the largest concentration dependent chemical shifts, correspond to residues located in the upper portions of helix 4 and 5, as illustrated in Figure 6. Although the exact dimer conformation cannot be concluded from the NMR titration data, the chemical shift changes observed are consistent with the dimer interface identified by X-ray crystallography (*19*). The concentration dependence of the amide resonances in HSQC spectra, when fit to a monomer/dimer model, provided

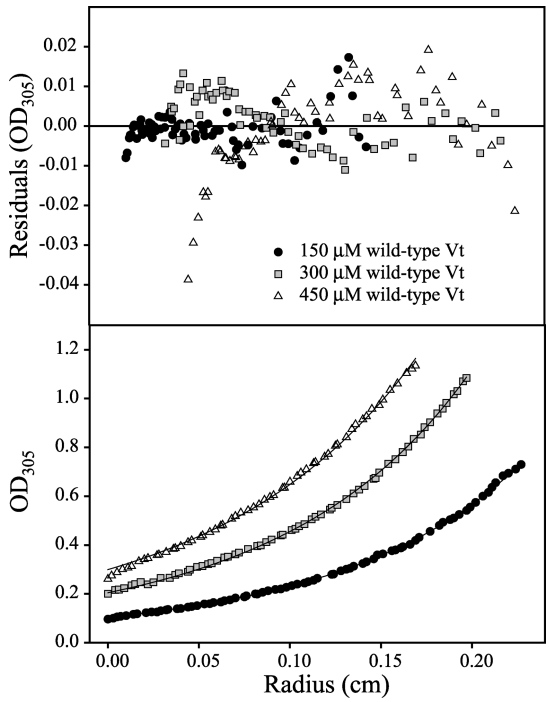


FIGURE 7: Analytical ultracentrifugation (AUC) studies conducted on both wild-type Vt and Vt H906A to quantify Vt self-association. Experiments were conducted at 150, 300, and 450 $\mu$M protein concentrations. Sedimentation equilibrium curves were fit to a monomer/dimer model, and a representative fit (wild-type Vt at pH 5.5) is shown. For clarity, the initial point of each curve was set to 0 cm. The $K_d$ for self-association was observed to be similar at pH 5.5 and pH 7.5 for both Vt and Vt H906A. In all cases, however, the association was relatively weak, with $K_d$ values of $\sim$300 $\mu$M. Dissociation constants determined for monomer/dimer fits are shown in Table 1.

Table 1

| | pH | $K_d$ ($\mu$M) | 95% confidence interval ($\mu$M) |
|---|---|---|---|
| wild-type Vt | 5.5 | 336 | 283−397 |
| wild-type Vt | 7.5 | 337 | 252−444 |
| Vt H906A | 5.5 | 323 | 271−382 |
| Vt H906A | 7.5 | 286 | 239−339 |

an approximate $K_d$ between 200 and 350 $\mu$M at pH 5.5. As the high protein concentrations required for NMR and complications associated with interpretation of chemical shifts can lead to significant uncertainty in the determination of a $K_d$, we conducted AUC to better characterize Vt self-association. Initial AUC studies, monitored at 280 nm using Vt samples between 10 and 40 $\mu$M, did not exhibit evidence of self-association (data not shown), consistent with the approximate $K_d$ obtained by NMR. However, AUC experiments conducted at higher protein concentrations show evidence of self-association for both wild-type Vt and Vt H906A (Figure 7). An apparent $K_d$ between 280 and 340 $\mu$M was obtained for both wild-type Vt and Vt H906A by fitting the AUC data to a monomer/dimer model. It remains unclear if the weak self-association for Vt observed in solution is physiologically relevant and whether it correlates with the Vt dimer induced in the presence of F-Actin (*32, 33*), as a model of F-Actin cross-linking by Vt, derived from electron microscopy and computational docking, suggested a distinct dimer from that of isolated Vt observed by NMR and X-ray crystallography (*32*). For both wild-type Vt and Vt H906A, there is also an increase in the residuals at the highest concentration (450 $\mu$M) when fitting to a monomer/dimer model. The increased residuals and their nonrandom nature at 450 $\mu$M may indicate higher order self-association. While the AUC data was fit to a monomer/dimer model, it is possible that Vt self-association may involve higher order oligomerization at higher concentrations, in which case, the $K_d$ values determined by a monomer/dimer fit may be inaccurate. Poor magnetization transfer efficiency in heteronuclear NMR experiments observed at higher concentrations (i.e., > 300 $\mu$M), provide additional support for higher order oligomerization. However, the nature and extent of this oligomerization is unclear.

In summary, our results show that the mutation of H906 to alanine does not significantly alter the conformation of Vt but may perturb interactions with the N-terminal strap. Moreover, our CD and NMR analyses do not support a pH dependent conformational change in Vt between pH 5.5 and 7.5. Furthermore, the H906A mutation does not appear to alter the response of Vt to changes in pH between 5.5 and 7.5. Finally, both wild-type Vt and Vt H906A can self-associate at pH 5.5 and 7.5, with a site of interaction consistent with the dimer interface identified by X-ray crystallography (*19*). The self-association is relatively weak in all cases, with monomer/dimer $K_d$ values of $\sim$300 $\mu$M. There is some evidence suggesting higher order oligomerization, but further research is needed to determine the nature of this oligomerization. As Vt dimerization has been previously implicated in F-Actin bundling, further research is warranted to elucidate the effect of ligand interactions on Vt self-association.

## ACKNOWLEDGMENT

We acknowledge Dr. Martin P. Playford for help with mutagenesis, Dr. Greg Young, the NMR facility manager at UNC-CH, for assistance in NMR data collection, and Dr. Ashutosh Tripathy, Director of the Macromolecular Interactions Facility, for assistance with CD and AUC.

## REFERENCES

1. Berrier, A. L., and Yamada, K. M. (2007) Cell-matrix adhesion. *J. Cell. Physiol. 213*, 565–573.
2. Danen, E. H., and Sonnenberg, A. (2003) Integrins in regulation of tissue development and function. *J. Pathol. 201*, 632–641.
3. Delon, I., and Brown, N. H. (2007) Integrins and the Actin cytoskeleton. *Curr. Opin. Cell Biol. 19*, 43–50.
4. Kedrin, D., van Rheenen, J., Hernandez, L., Condeelis, J., and Segall, J. E. (2007) Cell motility and cytoskeletal regulation in invasion and metastasis. *J. Mammary Gland Biol. Neoplasia 12*, 143–152.
5. Geiger, B., Tokuyasu, K. T., Dutton, A. H., and Singer, S. J. (1980) Vinculin, an intracellular protein localized at specialized sites where microfilament bundles terminate at cell membranes. *Proc. Natl. Acad. Sci. U.S.A. 77*, 4127–4131.
6. Xu, W., Baribault, H., and Adamson, E. D. (1998) Vinculin knockout results in heart and brain defects during embryonic development. *Development 125*, 327–337.
7. Coll, J. L., Ben-Ze'ev, A., Ezzell, R. M., Rodriguez Fernandez, J. L., Baribault, H., Oshima, R. G., and Adamson, E. D. (1995) Targeted disruption of vinculin genes in F9 and embryonic stem cells changes cell morphology, adhesion, and locomotion. *Proc. Natl. Acad. Sci. U.S.A. 92*, 9161–9165.
8. Huttelmaier, S., Bubeck, P., Rudiger, M., and Jockusch, B. M. (1997) Characterization of two F-Actin-binding and oligomerization sites in the cell-contact protein vinculin. *Eur. J. Biochem. 247*, 1136–1142.

9. Menkel, A. R., Kroemker, M., Bubeck, P., Ronsiek, M., Nikolai, G., and Jockusch, B. M. (1994) Characterization of an F-Actin-binding domain in the cytoskeletal protein vinculin. *J. Cell Biol. 126*, 1231–1240.
10. Wood, C. K., Turner, C. E., Jackson, P., and Critchley, D. R. (1994) Characterisation of the paxillin-binding site and the C-terminal focal adhesion targeting sequence in vinculin. *J. Cell Sci. 107* (Pt 2), 709–717.
11. Johnson, R. P., and Craig, S. W. (1994) An intramolecular association between the head and tail domains of vinculin modulates talin binding. *J. Biol. Chem. 269*, 12611–12619.
12. Johnson, R. P., and Craig, S. W. (1995) The carboxy-terminal tail domain of vinculin contains a cryptic binding site for acidic phospholipids. *Biochem. Biophys. Res. Commun. 210*, 159–164.
13. DeMali, K. A., Barlow, C. A., and Burridge, K. (2002) Recruitment of the Arp2/3 complex to vinculin: coupling membrane protrusion to matrix adhesion. *J. Cell Biol. 159*, 881–891.
14. Johnson, R. P., Niggli, V., Durrer, P., and Craig, S. W. (1998) A conserved motif in the tail domain of vinculin mediates association with and insertion into acidic phospholipid bilayers. *Biochemistry 37*, 10211–10222.
15. Ziegler, W. H., Tigges, U., Zieseniss, A., and Jockusch, B. M. (2002) A lipid-regulated docking site on vinculin for protein kinase C. *J. Biol. Chem. 277*, 7396–7404.
16. Weekes, J., Barry, S. T., and Critchley, D. R. (1996) Acidic phospholipids inhibit the intramolecular association between the N- and C-terminal regions of vinculin, exposing Actin-binding and protein kinase C phosphorylation sites. *Biochem. J. 314* (Pt 3), 827–832.
17. Miller, G. J., Dunn, S. D., and Ball, E. H. (2001) Interaction of the N- and C-terminal domains of vinculin. Characterization and mapping studies. *J. Biol. Chem. 276*, 11729–11734.
18. Bakolitsa, C., Cohen, D. M., Bankston, L. A., Bobkov, A. A., Cadwell, G. W., Jennings, L., Critchley, D. R., Craig, S. W., and Liddington, R. C. (2004) Structural basis for vinculin activation at sites of cell adhesion. *Nature 430*, 583–586.
19. Bakolitsa, C., de Pereda, J. M., Bagshaw, C. R., Critchley, D. R., and Liddington, R. C. (1999) Crystal structure of the vinculin tail suggests a pathway for activation. *Cell 99*, 603–613.
20. Chen, H., Choudhury, D. M., and Craig, S. W. (2006) Coincidence of Actin filaments and talin is required to activate vinculin. *J. Biol. Chem. 281*, 40389–40398.
21. Cohen, D. M., Chen, H., Johnson, R. P., Choudhury, B., and Craig, S. W. (2005) Two distinct head-tail interfaces cooperate to suppress activation of vinculin by talin. *J. Biol. Chem. 280*, 17109–17117.
22. Izard, T., Evans, G., Borgon, R. A., Rush, C. L., Bricogne, G., and Bois, P. R. (2004) Vinculin activation by talin through helical bundle conversion. *Nature 427*, 171–175.
23. Kelly, D. F., Taylor, D. W., Bakolitsa, C., Bobkov, A. A., Bankston, L., Liddington, R. C., and Taylor, K. A. (2006) Structure of the alpha-actinin-vinculin head domain complex determined by cryo-electron microscopy. *J. Mol. Biol. 357*, 562–573.
24. Miller, G. J., and Ball, E. H. (2001) Conformational change in the vinculin C-terminal depends on a critical histidine residue (His-906). *J. Biol. Chem. 276*, 28829–28834.
25. Borgon, R. A., Vonrhein, C., Bricogne, G., Bois, P. R., and Izard, T. (2004) Crystal structure of human vinculin. *Structure (Camb) 12*, 1189–1197.
26. Palmer, S. M., and Campbell, S. L. (2008) Backbone 1H, 13C and 15N NMR assignments of the tail domain of vinculin. *Biomol. NMR Assignments 2*, 69–71.
27. Cavanagh, J. (2007) *Protein NMR Spectroscopy: Principles and Practice*, 2nd ed., Academic Press, Amsterdam.
28. Delaglio, F., Grzesiek, S., Vuister, G. W., Zhu, G., Pfeifer, J., and Bax, A. (1995) NMRPipe: a multidimensional spectral processing system based on UNIX pipes. *J. Biomol. NMR 6*, 277–293.
29. Johnson, B. A., and Blevins, R. A. (1994) NMR View: A computer program for the visualization and analysis of NMR data. *J. Biomol. NMR 4*, 603–614.
30. Yphantis, D. A. (1964) Equilibrium Ultracentrifugation Of Dilute Solutions. *Biochemistry 3*, 297–317.
31. Kelly, S. M., Jess, T. J., and Price, N. C. (2005) How to study proteins by circular dichroism. *Biochim. Biophys. Acta 1751*, 119.
32. Janssen, M. E., Kim, E., Liu, H., Fujimoto, L. M., Bobkov, A., Volkmann, N., and Hanein, D. (2006) Three-dimensional structure of vinculin bound to Actin filaments. *Mol. Cell 21*, 271–281.
33. Johnson, R. P., and Craig, S. W. (2000) Actin activates a cryptic dimerization potential of the vinculin tail domain. *J. Biol. Chem. 275*, 95–105.
34. Izard, T., and Vonrhein, C. (2004) Structural basis for amplifying vinculin activation by talin. *J. Biol. Chem. 279*, 27667–27678.


BI801764A